Toward a mineral physics reference model for the Moon's core

Toward a mineral physics reference model for the Moon's core

Daniele Antonangeli[a,1], Guillaume Morard[a], Nicholas C. Schmerr[b], Tetsuya Komabayashi[c], Michael Krisch[d], Guillaume Fiquet[a], and Yingwei Fei[e]

[a]Institut de Minéralogie, de Physique des Matériaux, et de Cosmochimie, UMR CNRS 7590, Sorbonne Universités – UPMC, Muséum National d'Histoire Naturelle, IRD Unité 206, 75252 Paris, France; [b]Department of Geology, University of Maryland, College Park, MD 20742; [c]Department of Earth and Planetary Sciences, Tokyo Institute of Technology, Tokyo 152-8551, Japan; [d]European Synchrotron Radiation Facility, 38043 Grenoble Cedex, France; and [e]Geophysical Laboratory, Carnegie Institution of Washington, Washington, DC 20015

Edited by Ho-kwang Mao, Carnegie Institution of Washington, Washington, DC, and approved February 20, 2015 (received for review September 10, 2014)

The physical properties of iron (Fe) at high pressure and high temperature are crucial for understanding the chemical composition, evolution, and dynamics of planetary interiors. Indeed, the inner structures of the telluric planets all share a similar layered nature: a central metallic core composed mostly of iron, surrounded by a silicate mantle, and a thin, chemically differentiated crust. To date, most studies of iron have focused on the hexagonal closed packed (hcp, or ε) phase, as ε-Fe is likely stable across the pressure and temperature conditions of Earth's core. However, at the more moderate pressures characteristic of the cores of smaller planetary bodies, such as the Moon, Mercury, or Mars, iron takes on a face-centered cubic (fcc, or γ) structure. Here we present compressional and shear wave sound velocity and density measurements of γ-Fe at high pressures and high temperatures, which are needed to develop accurate seismic models of planetary interiors. Our results indicate that the seismic velocities proposed for the Moon's inner core by a recent reanalysis of Apollo seismic data are well below those of γ-Fe. Our dataset thus provides strong constraints to seismic models of the lunar core and cores of small telluric planets. This allows us to propose a direct compositional and velocity model for the Moon's core.

iron | high pressure | high temperature | Moon | telluric planetary cores

Even though the telluric planets and satellites have metallic cores composed mainly of iron, differences in bulk masses imply different pressure (P) and temperature (T) conditions at the center of these bodies. This, in turn, reflects on the solid versus liquid nature of the core and on the stable crystalline structure of the solid phase. The hexagonal closed-packed (hcp, or ε) phase is likely the stable Fe phase across the pressure and temperature conditions of Earth's core (1). At the moderate P–T characteristic of the cores of relatively small planets, such as Mercury (P between ∼8 GPa and ∼40 GPa, T between ∼1,700 K and ∼2,200 K) (2) or Mars (P between ∼24 GPa and ∼42 GPa, T between ∼2,000 K and 2,600 K) (3, 4), or satellites, including the Moon (P∼5–6 GPa, T between 1,300 K and 1,900 K) (5), the expected iron stable structure is face-centered cubic (fcc, or γ) (6). For this phase, there are not extensive experimental measurements of the aggregate sound velocities as a function of pressure and temperature. Studies are limited to a single determination of the Debye velocity at 6 GPa and 920 K (7) and to an inelastic neutron scattering (INS) experiment at ambient pressure and 1,428 K (8), although a complete and consistent set of measurements of compressional and shear wave sound velocities (respectively, V_P and V_S) and density (ρ) at high pressure and high temperature are essential parameters needed to develop reliable seismic models of planetary cores.

The Moon is the only other telluric body besides Earth for which multiple direct seismic observations are available. These were provided by the Apollo Lunar Surface Experiments Package (9) that, despite the very limited number of seismometers and the partial selenographical extent, provided precious information on the structure of the Moon's interior (10, 11). Nevertheless, seismic investigations of the deepest lunar interior (>900 km depth) remain very challenging. The structure of the lunar core is controversial, with only a single seismic study of core-reflected and converted S and P waves that directly detect the existence of a solid inner and a fluid outer core (10). The existence of a liquid outer core seems to be favored as well when considering polar moment of inertia, the overall elastic response to tidal potential (Love numbers), and mantle seismic constraints (10–12). In the analysis of the seismic data proposed in ref. 10, the inner core was modeled as pure iron, while the outer liquid core was modeled to contain less than 13 wt % of sulfur alloyed to iron (less than 6 wt % in the entire core). Various indirect observations also point to the existence of a metallic core (5, 12), although studies differ in many aspects, such as the radius of the core, the solid vs. liquid nature, or its composition. A precise determination of the structure and chemical composition of the Moon's core is essential for the understanding of present-day dynamics, as well as to constrain models of lunar origin and evolution, including the possible existence of a now-extinct lunar dynamo (5, 13).

The link between seismic observations and geophysical models can be provided by experiments that probe sound wave propagation in candidate materials at relevant thermodynamic conditions. Here we carried out density (ρ) and sound velocity (V_P and V_S) measurements on body-centered cubic (bcc) and fcc iron at simultaneous high pressure and high temperature, using

Significance

Iron is the main constituent of terrestrial planetary cores, taking on a hexagonal closed packed structure under the conditions of Earth's inner core, and a face-centered cubic (fcc) structure at the more moderate pressures of smaller bodies, such as the Moon, Mercury, or Mars. Here we present sound velocity and density measurements of fcc iron at pressures and temperatures characteristic of small planetary interiors. The results indicate that the seismic velocities currently proposed for the Moon's inner core are well below those of fcc iron or plausible iron alloys. Our dataset provides strong constraints to seismic models of the lunar core and cores of small telluric planets, and allows us to build a direct compositional and velocity model of the Moon's core.

Author contributions: D.A. designed research; D.A., G.M., T.K., M.K., G.F., and Y.F. performed research; D.A. and G.M. analyzed data; D.A., G.M., N.C.S., T.K., M.K., G.F., and Y.F. wrote the paper; N.C.S. performed core layering and moment of inertia modeling; and T.K. and Y.F. performed high-pressure cells setup.

The authors declare no conflict of interest.

This article is a PNAS Direct Submission.

[1]To whom correspondence should be addressed. Email: daniele.antonangeli@impmc.upmc.fr.

This article contains supporting information online at www.pnas.org/lookup/suppl/doi:10.1073/pnas.1417490112/-/DCSupplemental.

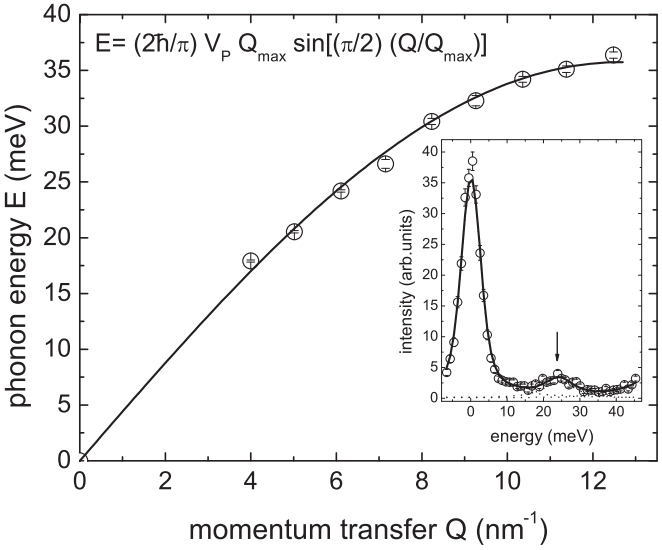

Fig. 1. Representative aggregate phonon dispersion obtained at 19 GPa and 1,100 K ($\rho = 8{,}620$ kg/m^3). The line is the best sine fit to the experimental data with V_P (the aggregate compressional sound velocity) and Q_{max} (the pseudo Brillouin boundary) left as free parameters. (*Inset*) Example of collected IXS spectra ($Q = 6.02$ nm^{-1}). The experimental data are shown together with the best-fit result (thick solid line) and the corresponding individual components (thin dotted lines). The arrow indicates the longitudinal acoustic phonon of iron. The rising slope at higher energies is the tail of the transverse acoustic phonon of diamond anvils.

inelastic X-ray scattering (IXS) combined with X-ray diffraction (XRD) measurements.

IXS allows a clear identification of longitudinal aggregate excitations in polycrystalline samples, the direct derivation of V_P, and the estimation of V_S (*SI Text, Inelastic X-Ray Scattering and Diffraction Measurements*) (Fig. 1). This technique has been proven very suitable for measurements on metallic samples compressed in diamond anvil cell (14–16), and has been recently extended for measurements under simultaneous high P–T conditions (17–20). Furthermore, combined XRD measurements yield an unambiguous phase determination and the direct derivation of the sample density (*SI Text, Inelastic X-Ray Scattering and Diffraction Measurements*).

Table 1. Summary of the collected data: pressure (P), temperature (T), density (ρ), observed phase, and compressional (V_P) and shear (V_S) sound velocity

P, GPa	T, K	ρ, kg/m^3	Phase	V_P, m/s	V_S, m/s
0	300	7,875	bcc	5920 ± 40	
2.5	800	7,790	bcc	5,900 ± 40	
3.1	300	7,975	bcc	6,030 ± 70	
3.3	1,020	7,700	bcc	5,660 ± 70	
7.3	800	8,000	bcc	6,120 ± 70	
0	1,150	7,560	fcc	5,220 ± 70	2,970 ± 150
7	1,000	8,105	fcc	6,080 ± 70	3,440 ± 180
10	1,100	8,205	fcc	5,920 ± 60	3,420 ± 180
19	1,100	8,620	fcc	6,590 ± 70	3,630 ± 200

P = 0 GPa and T = 300 K correspond to ambient P–T conditions. Temperature, density, and compressional sound velocity have been directly measured (*SI Text, Inelastic X-Ray Scattering and Diffraction Measurements*). Pressure has been measured only at 300 K (*SI Text, Inelastic X-Ray Scattering and Diffraction Measurements*); otherwise, it was derived from the equation of state (ref. 35 for the bcc phase and ref. 6 for the fcc phase). Shear velocities have been estimated combining measured V_P and ρ with bulk modulus from literature (6).

We collected data on pure Fe, for both bcc and fcc structures, covering a pressure and temperature range between 0 GPa and 19 GPa and 300 K and 1,150 K (Table 1 and Fig. 2). Within the quasi-harmonic approximation, the compressional sound velocity is expected to scale linearly with density (21), which allows us to compare results that were obtained at different pressure or temperature conditions. Both bcc and fcc phases show a linear V_P–ρ relationship over the investigated pressure and temperature range, similar to recently reported trends for the hcp phase over a comparable temperature range (18, 20). The sound velocity of the fcc phase is about 400 m/s lower than that of the bcc phase at the same density (Fig. 2). Such a difference is significantly larger than our error bars on V_P, which amount to about 1% (Table 1). Most importantly, the V_P value proposed for the Moon's inner core (10) after a reanalysis of Apollo lunar seismograms (4.3 km/s) is significantly below those of γ-Fe (Fig. 2). Such a large difference (~25% in V_P at constant density) is unlikely due to anharmonic high-temperature effects (*SI Text, Temperature Effects on the Sound Velocities*). Indeed, our measurements in the 1,000- to 1,150-K range compare well with INS measurements at ambient pressure and 1,428 K (8) and with measurements on fcc Fe–Ni alloys at high pressure and ambient temperature (17) (see Fig. 2), whereas the estimated temperature of the Moon's core is 1,300–1,900 K. Even the recent studies

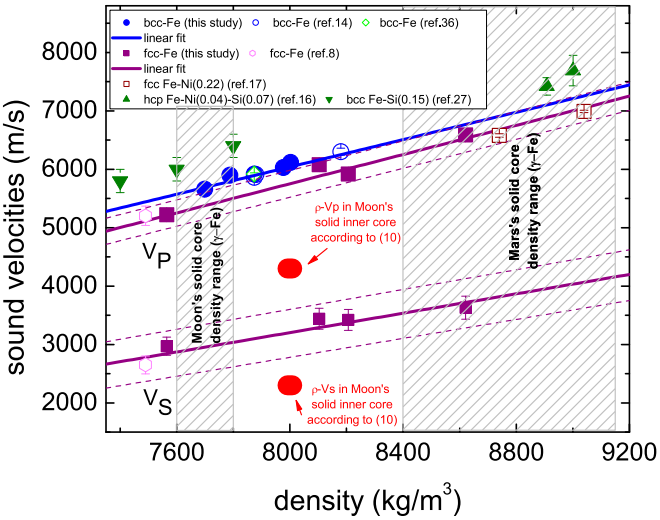

Fig. 2. Density evolution of the aggregate compressional (V_P) and shear (V_S) sound velocities. Solid circles, bcc Fe; open circles, bcc Fe from ref. 14; open diamond, ultrasonic determination on bcc Fe at ambient conditions (36). Solid squares, fcc Fe; open hexagon, INS on fcc Fe at ambient pressure and 1428 K (8); open squares, fcc $Fe_{0.78}Ni_{22}$ alloy (17). Solid triangles, hcp $Fe_{0.89}Ni_{0.04}Si_{0.07}$ alloy (16); upside-down triangles, bcc $Fe_{0.85}Si_{0.15}$ alloy (27). The experimental uncertainties on the densities are smaller than the symbol size. Error bars on the velocities account for the uncertainties related to the measured phonon energies, momentum transfer, and statistical errors of the fits (*SI Text, Inelastic X-Ray Scattering and Diffraction Measurements*). The lines are linear fits to the experimental data on pure Fe including the INS determination at ambient pressure ($V_P = a + b\rho$, with $a = -3{,}320 \pm 1{,}200$; $b = 1.17 \pm 0.15$ and $a = -4{,}250 \pm 700$; $b = 1.25 \pm 0.09$ for bcc Fe and fcc Fe, respectively). V_S for fcc Fe at 1,100 K ($V_S = a + b\rho$, with $a = -3{,}440 \pm 1{,}460$; $b = 0.83 \pm 0.18$) is estimated combining measured V_P with bulk moduli obtained by P–V–T equation of state (6). Dashed lines represent upper and lower bounds once considering possible effects coming from nonrandom averaging (up to ±5% for V_P and up to ±15% for V_S estimated as the difference between Voigt and Reuss averages), and combined uncertainties on the P–V–T equation of state (*SI Text, Inelastic X-Ray Scattering and Diffraction Measurements*). Density ranges for Moon and Mars solid core (modeled as pure γ-Fe after ref. 6) are crosshatched. The arrows point to V_P–ρ and V_S–ρ values proposed in ref. 10 for the Moon's solid core.

arguing for temperature effects report not more than ~5% softening in V_P in the hcp phase (19) and ~3% softening in V_P in the bcc phase (22), for a difference of 400 K.

The effects of frequency-dependent viscoelastic relaxation are more difficult to address, as anelasticity is a very complex issue that requires detailed knowledge of the material data at exact conditions (P–T conditions, grain size, impurities, defects, etc.), and are very often neglected. General consensus is that viscoelastic relaxation is more relevant for V_S than for V_P. Even for V_S, assuming a seismic quality factor Q of ~100 (23) and a frequency dependence α of ~0.1–0.3 for the Moon's core (24), the expected sound velocity reduction is only 1–3%.

We also examine the possibility of iron alloyed with nickel and/or other lighter elements. The effects on sound velocities when alloying other elements to solid iron have been widely investigated, both experimentally (16, 17, 19, 25–27) and theoretically (28, 29). As a first approximation, we assume the same qualitative behavior for all iron structures and look at likely candidates with respect to their cosmochemical abundances and chemical affinity. Nickel incorporation of up to 22 atomic % (at.%) slightly increases density at the same pressure (30) but does not change the compressional sound velocity (17) (Fig. 2). Inclusion of light elements such as silicon, sulfur, or carbon can significantly reduce the density, but the compressional sound velocity at constant density is shown to increase (16, 19, 25–28) (Fig. 2). $FeTiO_3$ ilmenite has been argued as a possible phase in the lunar core, in particular in models assuming a large core size (12), but this oxide is stiffer than metallic iron (31), which would yield even larger sound velocities at the appropriate density for this compound.

Thus, the sound velocity proposed for the Moon's inner core (10) is incompatible with that of pure solid iron or any plausible solid iron alloys. Nonetheless, seismic data analysis and refinements of the lunar moment of inertia require the Moon to have an inner solid core and an outer liquid core. Here we use our results to construct mineral physical constraints on this lunar core model, reinterpreting the seismic observations (10) on the basis of our experimental measurements of V_P, V_s, and ρ.

When considering iron and iron alloys phase diagrams, the temperatures characteristic of the Moon's interior point to the Fe–FeS system as the most probable explanation for a liquid iron alloy stable at the thermodynamic conditions of the Moon's core (13). To have a solid inner core, pure Fe has to be the solid phase coexisting with Fe–FeS melt at the liquidus. The Fe–FeS phase diagram at 5 GPa indicates that pure Fe can be at equilibrium with liquid Fe–S only if the S content is lower than ~37 at.% (Fig. S1). The temperature imposes further constraints: if partial melting is present at the bottom of the mantle (10, 32), temperatures at the core–mantle boundary (CMB) must exceed 1,650 K. The temperature at the inner core/outer core boundary (ICB) may be only a few tens of degrees higher than that at CMB, if we assume a nonconvective subadiabatic liquid, an assumption compatible with the absence of an active lunar dynamo (33). For temperatures at the ICB of at least 1,700 K, the amount of sulfur in the liquid phase could be brought down to 20 at.%, and even less for higher temperatures (Fig. S1). In this scenario, our best estimates (*SI Text, Density and Sound Velocity for Fe–S Liquid Alloy*) of the density (Fig. S2) and the corresponding velocity for the outer core (with a sulfur content ranging from 10 at.% to 20 at.%, P of ~5 GPa, and T of ~1,800 K) are 6,500–7,000 kg/m^3 and 3,500–4,100 m/s. Irrespective of the outer core composition, an inner core made of pure γ-Fe, with density of 7,600–7,800 kg/m^3 (6), will have compressional velocities between 4,750 and 5,700 m/s, and shear velocities between 2,150 and 3,450 m/s (Fig. 2), even when accounting for up to ~5% reduction in V_P and ~10% reduction in V_S at constant density due to possible anharmonic effects when scaling up temperatures to 1,900 K (*SI Text, Temperature Effects on the Sound Velocities*). Our proposed velocity and density model for the Moon's core is shown in Fig. 3 and summarized in Table S1.

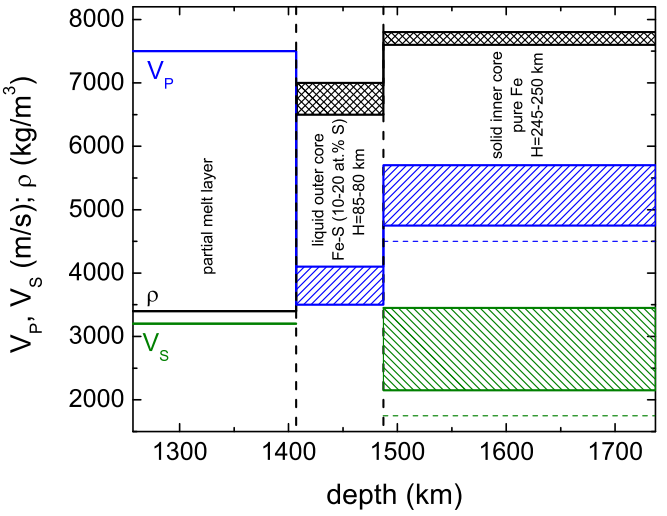

Fig. 3. Preferred velocity (V_P, V_S), density (ρ) and compositional model for the Moon's core. Constraints on the partial melt layer are from ref. 10. Shaded areas represent uncertainties on our values. Horizontal dashed lines are lower bounds for V_P and V_S when considering possible strong premelting effects in the inner core (*SI Text, Temperature Effects on the Sound Velocities*). Frequency-dependent viscoelastic effects have been neglected. The inner core–outer core boundary is assumed to be at ~5 GPa and ~1,800 K.

Taking into account these mineral physics constraints and the seismic travel times reported in ref. 10, we can estimate inner core and outer core sizes (*SI Text, Core Layering Modeling Methods*). We obtain an inner core having a radius of ~245–250 km and an outer core ~85–80 km thick (Fig. 3). The total amount of sulfur in the core shell would then be between ~3 and ~6 wt %, as a result of the mass balance between the sulfur-bearing liquid outer core (10–20 at.%, corresponding to 6–11 wt %) and the pure iron solid inner core. This independent estimate is in excellent agreement with very recent modeling of lunar core formation and metal/silicate partitioning of siderophile elements (34), resulting in a Moon core containing up to 6 wt % S, and compatible with requirements from a long-lived lunar dynamo modeling, calling for 6–8 wt % S in the Moon's core (13). We further validate the direct model proposed here by comparison with Moon's observables such as mass and moment of inertia, finding values that fall within 0.1% of known values (*SI Text, Moment of Inertia Modeling Methods*).

Finally, our results can easily be extrapolated to the conditions of telluric planetary cores up to Mars size (Fig. 2). V_P of γ-Fe at 42 GPa and 2,500 K (ρ of ~9,100 kg/m^3), P–T expected at the center of Mars, should be ~7,100 m/s; and V_P of γ-Fe at 40 GPa and 2,200 K (ρ of ~8,900 kg/m^3), P–T expected at the center of Mercury, should be ~6,800 m/s. More delicate is the extrapolation of V_S, which can be estimated for both cases in the 3,600–4,400 m/s range. Seismic records for Mars are not available yet, but the main objective of the InSight NASA Discovery mission (launch in March 2016) is to place a seismic station for the study of Martian interior structure (solarsystem.nasa.gov/insight/home.cfm). Our results and similar datasets will be fundamental to the interpretation of such seismic observations, as well as for direct modeling of solid cores of small telluric planets.

ACKNOWLEDGMENTS. We acknowledge M. Mezouar for spectroradiometric measurements and J. Siebert for discussions. This work was supported by French National Research Agency Grant 2010-JCJC-604-01 (to D.A.) and Grant ANR-12-BS04-0015-04 (to G.M.) and by NASA Grant NNX14AG26G (to Y.F.) and Grant NNX09AO80G (to N.C.S.). D.A. also acknowledges financial support from the PNP program of CNRS-INSU.

1. Tateno S, Hirose K, Ohishi Y, Tatsumi Y (2010) The structure of iron in Earth's inner core. *Science* 330(6002):359–361.
2. Chen B, Li J, Hauck SA (2008) Non-ideal liquidus curve in the Fe-S system and Mercury's snowing core. *Geophys Res Lett* 35:L07201.
3. Bertka CM, Fei Y (1998) Implications of Mars Pathfinder data for the accretion history of the terrestrial planets. *Science* 281(5384):1838–1840.
4. Fei Y, Bertka C (2005) Planetary science. The interior of Mars. *Science* 308(5725): 1120–1121.
5. Wieczorek MA, et al. (2006) The constitution and structure of the lunar interior. *Rev Mineral Geochem* 60:221–364.
6. Tsujino N, et al. (2013) Equation of state of γ-Fe: Reference density for planetary cores. *Earth Planet Sci Lett* 375:244–253.
7. Shen G, et al. (2004) Phonon density of states in iron at high pressures and high temperatures. *Phys Chem Miner* 31:353–359.
8. Zarestky J, Stassis C (1987) Lattice dynamics of γ-Fe. *Phys Rev B Condens Matter* 35(9): 4500–4502.
9. Nakamura Y, Latham GV, Dorman HJ (1982) Apollo lunar seismic experiment:—Final summary. *J Geophys Res* 87(S01):A117–A123.
10. Weber RC, Lin PY, Garnero EJ, Williams Q, Lognonné P (2011) Seismic detection of the lunar core. *Science* 331(6015):309–312.
11. Garcia RF, Gagnepain-Beyneix J, Chevrot S, Lognonné P (2011) Very preliminary reference Moon model. *Phys Earth Planet Inter* 188:96–113, and correction (2012) 202-203: 89–91.
12. Lognonné P, Johnson C (2007) Planetary seismology. *Treatise Geophys.* 10:69–122.
13. Laneuville M, et al. (2014) A long-lived lunar dynamo powered by core crystallization. *Earth Planet Sci Lett* 401:251–260.
14. Fiquet G, Badro J, Guyot F, Requardt H, Krisch M (2001) Sound velocities in iron to 110 gigapascals. *Science* 291(5503):468–471.
15. Antonangeli D, et al. (2004) Elastic anisotropy in textured hcp-iron to 112 GPa from sound wave propagation measurements. *Earth Planet Sci Lett* 225:243–251.
16. Antonangeli D, et al. (2010) Composition of the Earth's inner core from high-pressure sound velocity measurements in Fe–Ni–Si alloys. *Earth Planet Sci Lett* 295(1-2): 292–296.
17. Kantor AP, et al. (2007) Sound wave velocities of fcc Fe–Ni alloy at high pressure and temperature by mean of inelastic X-ray scattering. *Phys Earth Planet Inter* 164(1-2): 83–89.
18. Antonangeli D, et al. (2012) Simultaneous sound velocity and density measurements of hcp iron up to 93 GPa and 1100 K: An experimental test of the Birch's law at high temperature. *Earth Planet Sci Lett* 331-332:210–214.
19. Mao Z, et al. (2012) Sound velocities of Fe and Fe–Si alloy in the Earth's core. *Proc Natl Acad Sci USA* 109(26):10239–10244.
20. Ohtani E, et al. (2013) Sound velocity of hexagonal close-packed iron up to core pressures. *Geophys Res Lett* 40:5089–5094.
21. Birch F (1961) Composition of the Earth's mantle. *Geophys J R Astron Soc* 4:295–311.
22. Liu J, Lin JF, Alatas A, Bi W (2014) Sound velocities of bcc-Fe and $Fe_{0.85}Si_{0.15}$ alloy at high pressure and temperature. *Phys Earth Planet Inter* 233:24–32.
23. Nakamura Y, et al. (1973) New seismic data on the state of the deep lunar interior. *Science* 181(4094):49–51.
24. Jackson I, Fitz Gerald JD, Kokkonen H (2000) High-temperature viscoelastic relaxation in iron and its implications for the shear modulus and attenuation of the Earth's inner core. *J Geophys Res* 105(B10):23605–23634.
25. Badro J, et al. (2007) Effect of light elements on the sound velocities in solid iron: Implications for the composition of the Earth's core. *Earth Planet Sci Lett* 254: 233–238.
26. Fiquet G, Badro J, Gregoryanz E, Fei Y, Occelli F (2009) Sound velocity in iron carbide (Fe_3C) at high pressure: Implications for the carbon content of the Earth's inner core. *Phys Earth Planet Inter* 172:125–129.
27. Lin JF, et al. (2003) Sound velocity of iron-nickel and iron-silicon alloys at high pressure. *Geophys Res Lett* 30(21):2112.
28. Vočadlo L (2007) Ab initio calculations of the elasticity of iron and iron alloys at inner core conditions: Evidence for a partially molten inner core? *Earth Planet Sci Lett* 254: 227–232.
29. Mookherjee M (2011) Elasticity and anisotropy of Fe_3C at high pressure. *Am Mineral* 96:1530–1536.
30. Mao HK, Wu Y, Chen LC, Shu J, Jephcoat AP (1990) Static compression of iron to 300 GPa and $Fe_{0.8}Ni_{0.2}$ alloy to 260 GPa: Implications for composition of the core *J Geophys Res* 95(B13):21737–21742.
31. Tronche EJ, et al. (2010) The thermal equation of state of $FeTiO_3$ ilmenite based on in situ X-ray diffraction at high pressures and temperatures. *Am Mineral* 95:1708–1716.
32. van Kan Parker M, et al. (2012) Neutral buoyancy of titanium-rich melts in the deep lunar interior. *Nat Geosci* 5:186–189.
33. Williams Q (2009) Bottom-up versus top-down solidifications of the cores of small solar system bodies: Constraints on paradoxical cores. *Earth Planet Sci Lett* 284: 564–569.
34. Rai N, van Westrenen W (2014) Lunar core formation: New constraints from metal-silicate partitioning of siderophile elements. *Earth Planet Sci Lett* 388:343–352.
35. Huang E, Bassett WA, Tao P (1987) Pressure-temperature-volume relationship for hexagonal closed packed iron determined by synchrotron radiation. *J Geophys Res* 92(B8):8129–8135.
36. Guinan MW, Beshers DN (1968) Pressure derivatives of the elastic constants of α-iron to 10 kbs. *J Phys Chem Solids* 29:541–549.